

Supporting Information

Mild Continuous Hydrogenolysis of Kraft Lignin over Titanium Nitride-Nickel Catalyst

*Valerio Molinari, Gylhaine Clavel, Micaela Graglia, Markus Antonietti and Davide
Esposito**

Author Address: Max-Planck-Institute of Colloids and Interfaces, 14424 Potsdam, Germany.

*Corresponding author: davide.esposito@mpikg.mpg.de

Table of Content:

Figures:

Figure S 1: XRD of TiN and TiN-Ni composites, showing the peak position shift of TiN in 220 plane (left) and the absence of the shift in Ni phase (right).	6
Figure S 2: diffraction of TiN and TiN-Ni with different loading of Ni.	7
Figure S 3: diffraction of TiN (a) and TiN pyrolyzed in the presence of acetic acid (b), sodium acetate (c), ammonium acetate (d) and no additive (e).	7
Figure S 4: Ni size distribution in the TiO ₂ -Ni (50%) composite.	8
Figure S 5: Ni size distribution in the TiN-Ni (50%) composite.	9
Figure S 6: SEM (left) and corresponding EDX-Mapping (right) of TiN-Ni (50%); Average size of Ni nanoparticle dispersed on TiN: ~68 nm	9
Figure S 7: SEM and corresponding EDX-Mapping of TiO ₂ -Ni (50%)	10
Figure S 8: 2D HSQC NMR analysis of fraction 1 of depolymerised lignin (Table 2, entry 3)	13
Figure S 9: 2D HSQC NMR analysis of acetylated kraft lignin (kraft lignin was acetylated before NMR analysis to improve its solubility).	14
Figure S 10: molecules used as standard for the identification of the monomers produced via lignin hydrogenolysis.	15
Figure S 11: GC-FID chromatograms of the depolymerized mixtures (fraction 1) obtained after lignin hydrogenation at 150 °C using Pd/C, TiO ₂ -Ni (50%) and TiN-Ni (50%) as catalysts.	16
Figure S 12: GC-MS chromatograms of the depolymerized mixtures (fraction 1) obtained after lignin hydrogenation at 150 °C using TiN-Ni (50%) and RaNi as catalysts. Samples injected without derivatisation	17
Figure S 13: SEM of TiN-Ni recovered after 500 hours of lignin hydrogenolysis (A), and high magnification (B).	18
Figure S 14: normalized yields for 2-Methoxy-4-propylphenol (Figure 6A, peak at 13 min) as a function of the time. The sample was injected without derivatisation of the –OH functional groups. .	18
Figure S 15: normalized yields for Homovanillyl alcohol (Figure 6A, peak at 16 min). The sample was injected without derivatisation of the –OH functional groups	19
Figure S 16: Nitrogen sorption analysis and specific surface area (BET) of fresh and recovered Pd/C (A) and corresponding pore size distributions (B)	19
Figure S 17: screenshot of the flow system control panel indicating the pressure reached by the system (1) and the pressure set by the user (2) (A). RaNi leakage after 40 hours of reaction (B).	20
Figure S 18: diffractogram (A) and FTIR (B) of the powder leaked from RaNi catalytic bed.	20

Figure S 19: Nitrogen atomic content quantified by Electron Energy Loss Spectroscopy in TiN prepared via urea route and on TiON and TiN reference samples.	21
Figure S 20: FTIR of pristine and reacted lignin.	21
Figure S 21: Diffractogram of TiN prepared via urea route.	22
Figure S 22: Size Exclusion Chromatography of reacted lignin after reaction (Table 2, entry 2, Fraction 1)	22
Figure S 23: Size Exclusion Chromatography of reacted lignin after reaction (Table 2, entry 2, Fraction 2)	23
Figure S 24: Size Exclusion Chromatography of reacted lignin after reaction (Table 2, entry 2, Fraction 3)	23
Figure S 25: Size Exclusion Chromatography of reacted lignin after reaction (Table 2, entry 3, Fraction 1)	24
Figure S 26: Size Exclusion Chromatography of reacted lignin after reaction (Table 2, entry 5, Fraction 1)	24
Figure S 27: Size Exclusion Chromatography of reacted lignin after reaction (Table 2, entry 5, Fraction 2)	25
Figure S 28: Size Exclusion Chromatography of reacted lignin after reaction (Table 2, entry 9, Fraction 1)	25
Figure S 29: Size Exclusion Chromatography of reacted lignin after reaction (Table 2, entry 13, fraction 1)	26
Figure S 30: Size Exclusion Chromatography of reacted lignin after reaction (Table 2, entry 13, fraction 2)	26
Figure S 31: Size Exclusion Chromatography of reacted lignin after reaction (Table 2, entry 14, fraction 1)	27
Figure S 32: Size Exclusion Chromatography of reacted lignin after reaction (Table 2, entry 14, fraction 2)	27

Tables:

Table S 1: cell parameters calculated from the (200) plane and d spacing shift calculated for all the planes of TiN phase.	7
Table S 2: change in d spacing after Ni loading calculated for all the diffraction planes of TiN phase.	8
Table S 3: combustion elemental analysis of TiX and TiX-Ni materials.	8
Table S 4: FTIR data analysis of unreacted lignin	11

Table S 5: solubility tests on kraft lignin: 200 mg of kraft lignin were stirred in 100 mL of solvent, after 48 hours the solvent was filtered and the precipitated lignin was weighted to calculate the concentration of biopolymer dissolved, the lignin dissolved was also isolated and weighted after drying of the solvent. ^aTHF = tetrahydrofuran, GVL = γ -valerolactone, meTHF = 2-methyltetrahydrofuran. 11

Table S 6: size exclusion chromatography and detected molecular weight of unreacted and reacted lignin after chromatographic column. Please refer to Table 2 in the manuscript for information regarding the depolymerisation conditions. 12

Table S 7: cumulative percent area for regions A, B and C (as defined in Comments on Figure S11) in the GC-FID chromatograms for the hydrogenolysis of lignin with different catalysts (Table 2) 17

Supporting information:

Materials:

Titanium (IV) chloride, benzyl phenyl ether (98%), urea, nickel (II) acetate tetrahydrate, alkali lignin, Pd/C (10%), methanol and ethanol were purchased from Sigma Aldrich and used as received. Raney Nickel packed cartridge was purchased from ThalesNano.

Methods:

Wide angle diffraction measurements (XRD) were performed using a Bruker D8 diffractometer equipped with Cu-K α source ($\lambda = 0.154$ nm) and a scintillation counter. All the reference patterns used can be found in the ICDD PDF-4+ database (2014 edition). TEM images were taken using a Zeiss EM 912 Ω microscope operated at an acceleration voltage of 120 kV; while the HR-TEM, measurements were recorded using a CM200FEG (Philips) microscope operated at 200 kV. SEM pictures were taken using a LEO 1550 Gemini microscope. Gas (nitrogen) sorption experiments were done using Quantachrome Quadrasorb apparatus. The samples were degassed (150 °C, 20 hours) before the experiments and the results were analysed with QuadraWin software (version 5.05). FT-IR spectra were recorded on a Varian1000-FT-IR spectrometer. Elemental analysis was performed as combustion analysis using a Vario Micro device. ¹H- and ¹³C-NMR spectra were acquired using a Bruker Spectrospin 400 MHz Ultrashield Spectrometer in deuterated solvents. 2D HSQC NMR were acquired using an Agilent 400 MHz Spectrometer in deuterated solvents. SEC (Size exclusion chromatography) with UV/RI detection was performed using N-methyl-2-pyrrolidone as eluent at 70°C using two PSS-GRAM columns (300 mm, 8 mm²) with an average particle size of 7 μ m and porosity between 100–1000 Å. Polystyrene was used as standard for the calibration. Conversions and yields for lignin reaction were calculated by mass difference after liquid chromatographic separation. GC-MS analyses were performed using an Agilent Technologies 5975 gas chromatograph equipped with a 1) MS detector and a capillary column (HP-5MS, 30 m, 0.25 mm, 0.25 micron) on the front inlet, and 2) FID detector in combination with a second HP-5MS capillary column on the back inlet. For benzyl phenyl ether the temperature program started with an isothermal step at 50 °C for 2 min, in a second step the temperature was increased to 300 °C (rate of 30 °C/min) and then kept for 1 min. For lignin and reacted lignin the temperature program started with an isothermal step at 50 °C for 2 min, in a second step the temperature was increased to 300 °C (rate of 10 °C/min) and then kept for 20 min. The injector temperature is kept at 250 °C and the detector at 280 °C.

TiN preparation:

Following a reported procedure, titanium tetrachloride (1156 μ L, 10.53 mmol) was added dropwise to ethanol (5 mL), to form a yellowish solution. Urea (2.61 g, 42.11 mmol) was added slowly to the solution forming a homogeneous yellow gel. The gel was heated under nitrogen flow (heating ramp of 2 K min⁻¹) up to 750 °C holding the final temperature (750 °C) for an additional 3 hours, then allowed to cool down to room temperature. The resulting bronze powder was analyzed by XRD (compared to 00-038-1420, PDF4 database) and used as such.

TiN-Ni preparation:

Nickel acetate tetrahydrate (1, 10, 20, 50 mol % with respect to TiN) was dissolved in ethanol (10 mL) and added dropwise to titanium nitride (0.864 g, 13.32 mmol). The suspension was stirred overnight, thus the solvent was slowly evaporated under nitrogen flow, obtaining a homogeneous bronze powder. The powder was heated under nitrogen flow (heating ramp of 2 K min⁻¹) holding the final temperature (475 °C) for 3 hours. The resulting magnetic powders were analyzed by XRD and used as such.

TiO₂ preparation:

Titanium tetrachloride (1156 μL, 10.53 mmol) was added dropwise to ethanol (5 mL), resulting in a yellowish solution. Urea (2.61 g, 42.11 mmol) was added slowly to the solution forming a homogeneous yellow gel. The gel was then heated under air atmosphere (heating ramp of 2K min⁻¹) up to 500 °C holding the final temperature for an additional 3 hours. The resulting powder was analyzed by XRD and used as such.

TiO₂-Ni preparation:

Nickel acetate tetrahydrate (0.84 g, 3.13 mmol) was dissolved in ethanol (15 mL) and added dropwise to titanium oxide (0.50 g, 6.25 mmol). The suspension was stirred overnight, and then the solvent was slowly evaporated under nitrogen flow, obtaining a homogeneous powder. The powder was heated under nitrogen flow (heating ramp of 2 K min⁻¹) holding the final temperature (475 °C) for 3 hours. The resulting magnetic powders were analysed by XRD and used as such.

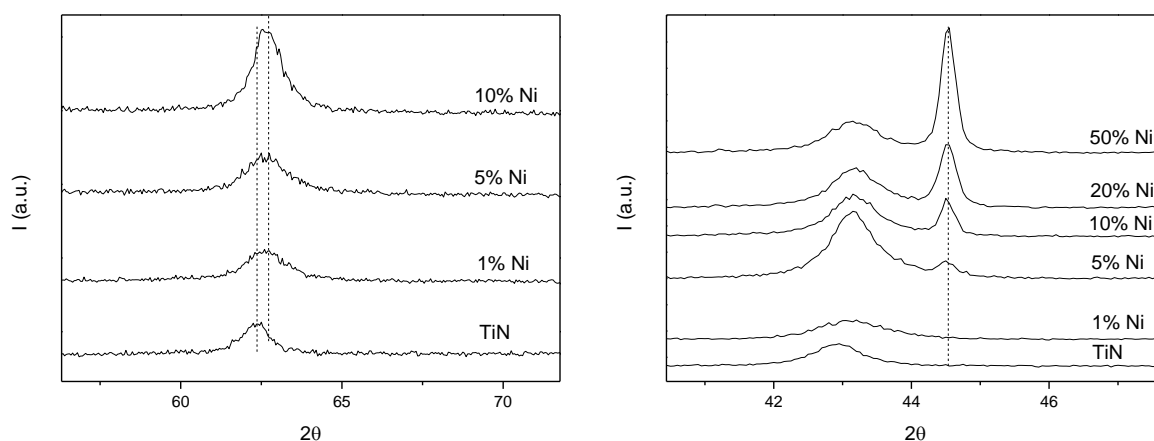


Figure S 1: XRD of TiN and TiN-Ni composites, showing the peak position shift of TiN in 220 plane (left) and the absence of the shift in Ni phase (right).

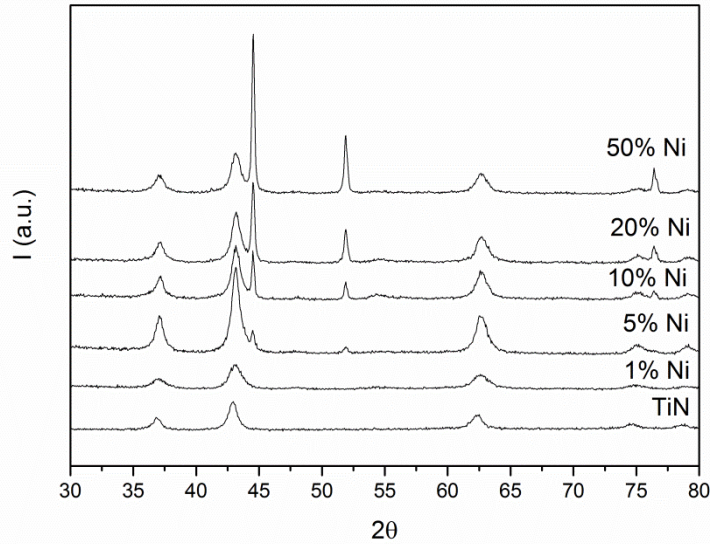


Figure S 2: diffraction of TiN and TiN-Ni with different loading of Ni.

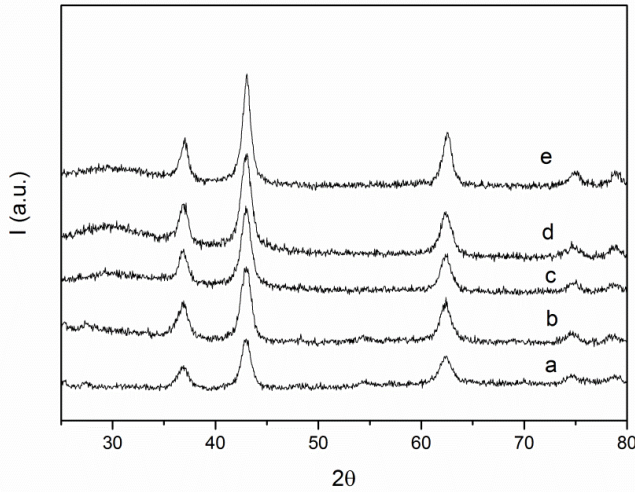


Figure S 3: diffraction of TiN (a) and TiN pyrolyzed in the presence acetic acid (b), sodium acetate (c), ammonium acetate (d) and no additive (e).

Table S 1: cell parameters calculated from the (200) plane and d spacing shift calculated for all the planes of TiN phase.

Sample	d (Å)	a (Å)
TiN	2,1042	4,2085
TiN-Ni 1%	2,0938	4,1877
TiN-Ni 5%	2,0936	4,1873
TiN-Ni 10%	2,0924	4,1849
TiN-Ni 20%	2,0906	4,1813
TiN-Ni 50%	2,0906	4,1812
c-TiN	2,1204	4,2408
c-TiN-Ni (50%)	2,1181	4,2363
c-TiC	2,1637	4,3274
c-TiC-Ni (50%)	2,1621	4,3242

Table S 2: change in d spacing after Ni loading calculated for all the diffraction planes of TiN phase.

Plane	d spacing TiN (Å)	d spacing TiN-Ni 1% (Å)	d spacing TiN-Ni 50% (Å)	Δd TiN-TiN1% (Å)	Δd TiN-TiN50% (Å)
111	2.4293	2.4227	2.4173	0.0066	0.0120
200	2.1042	2.0938	2.0896	0.0104	0.0146
202	1.4882	1.4826	1.4795	0.0056	0.0087
311	1.2686	1.2642	-	0.0044	-
222	1.2158	1.2118	-	0.0040	-

Table S 3: combustion elemental analysis of TiX and TiX-Ni materials.

Sample	N (wt%)	C (wt%)	O (wt%)	N/O ratio (wt)
TiN	14.2	5.4	7	2.08
TiN-Ni (1%)	13.0	7.3	6.6	1.97
TiN-Ni (5%)	12.6	7.6	6.8	1.85
TiN-Ni (10%)	11.3	6.7	5.8	1.95
TiN-Ni (20%)	10.7	7.2	5.4	1.98
TiN-Ni (50%)	6.6	8.9	3.2	2.06
TiON (reference)	-	-	15	-
TiN (reference)	16.5	0.2	-	-
TiO ₂	0.6	0.3	Not measured	-

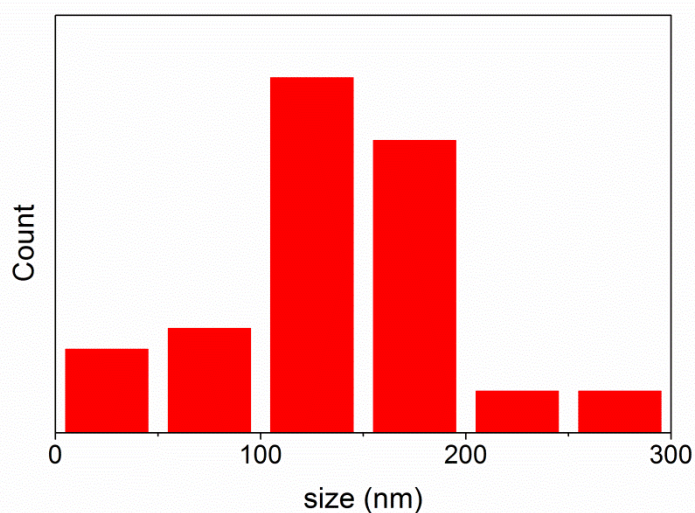


Figure S 4: Ni size distribution in the TiO₂-Ni (50 %) composite.

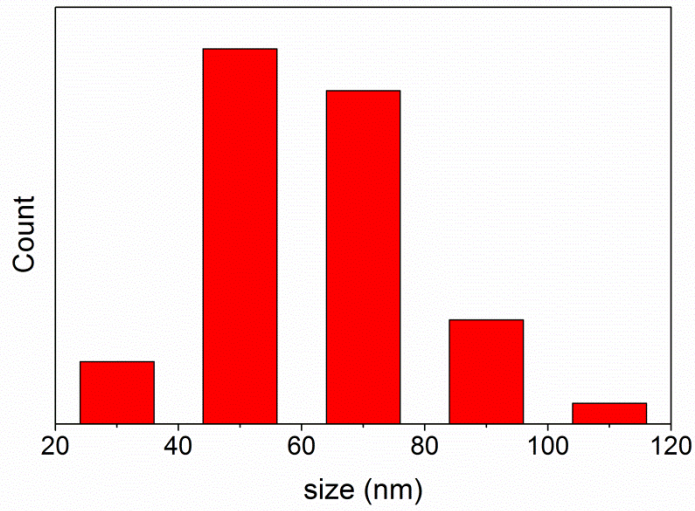


Figure S 5: Ni size distribution in the TiN-Ni (50 %) composite.

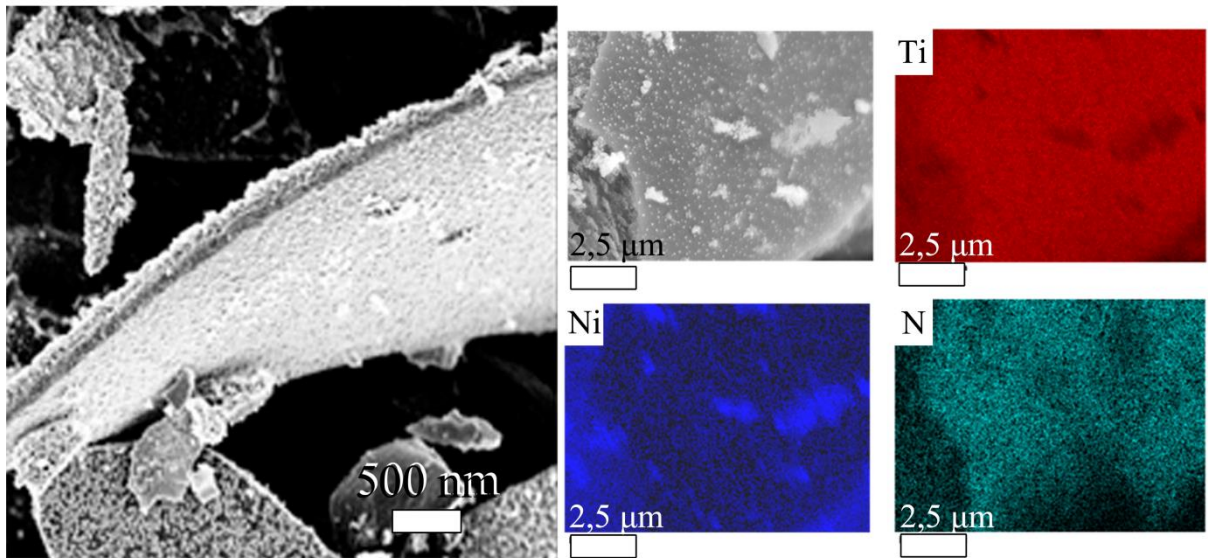


Figure S 6: SEM (left) and corresponding EDX-Mapping (right) of TiN-Ni (50 %); Average size of Ni nanoparticle dispersed on TiN: ~68 nm.

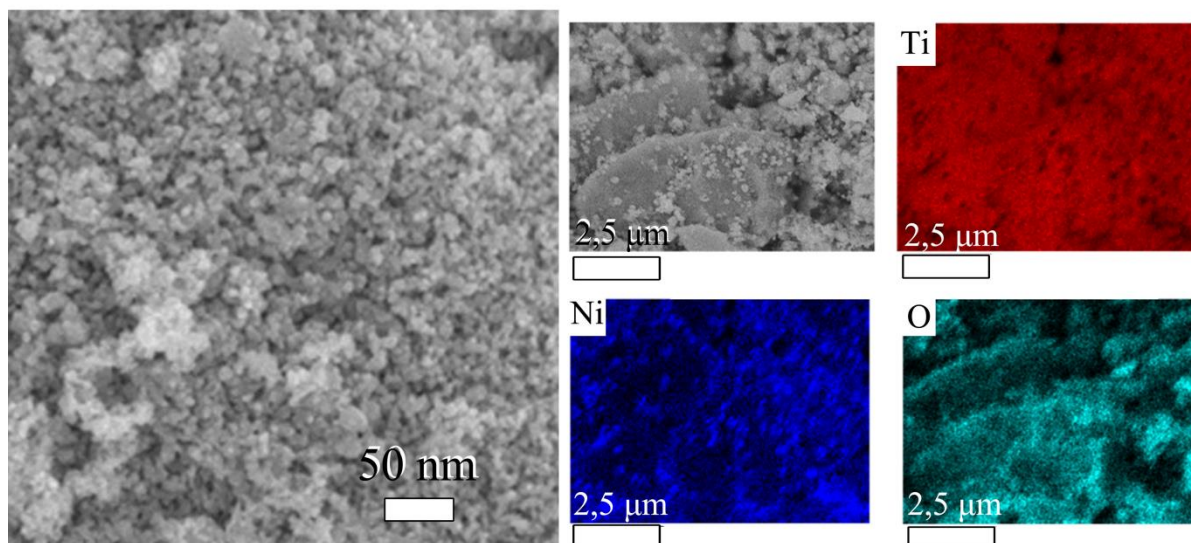


Figure S 7: SEM and corresponding EDX-Mapping of TiO₂-Ni (50 %).

Continuous hydrogenolysis reactions:

All the hydrogenolysis reactions were performed using a H-Cube ProTM reactor. The catalysts were packed in a stainless steel column (70 mm). Filtered solutions of the starting materials (benzyl phenyl ether or lignin) in the appropriate solvent were pumped into the reactor, which mixes the liquid with a feed of hydrogen successively passing through the column containing the catalyst. The residence time inside the column was controlled varying the flow rate. The pressure of the system was set to 12 bars for benzyl phenyl ether and increased to 25 bars for lignin reactions.

Liquid Chromatography of reacted lignin:

Reacted lignin was collected as the eluate of the reactor and the solvent was evaporated under vacuum. The obtained crude was then separated in different fractions through silica chromatography (6 grams of silica were used for 100 mg of crude reacted lignin). The first fraction was eluted using 300 mL of a mixture of n-hexane/isopropanol/methanol (75/20/5, 300 mL). The second fraction was eluted using ethanol (300 mL) while unreacted material was recovered from the silica eluting with methanol (300 mL).

Derivatization of depolymerised lignin:

15 mg of dried sample are dissolved in 125 μL of CHCl₃ and 250 μL of BSTFA (Supelco, Sigma Aldrich) are added to the solution. The mixture is heated at 70 °C, after 45 minutes it is cooled down to room temperature and injected in the GC-MS system. Guaiacol, vanillin, oleic acid, vanillic acid and homovanillyl alcohol (Sigma Aldrich) are identified by GC-MS comparison with the corresponding pure standard. In order to identify the hydrogenated coniferil alcohol, the corresponding standard was prepared as follow: a solution of commercial coniferil alcohol (Sigma Aldrich) in MeOH is fluxed through a Pd/C (10%) filled

cartridge with a flow of 0.5 ml/min in the presence of hydrogen, at 30°C and 20 bar in the H-Cube Pro™ reactor. All the other monoaromatics were identified by NIST05a library.

Table S 4: FTIR data analysis of unreacted lignin

Signal	Corresponding vibration ^{30,31}
3565–3116	Phenolic and alcoholic OH stretching vibrations
2987–2854	C-H stretching of methoxy groups
2854–2802	C-H stretching of methoxy groups
1625–1553	Aromatic ring vibration
1530–1477	
1473–1436	Aromatic ring vibration + CH ₂ and CH methoxy
1436–1401	
1380–1346	Phenolic hydroxyls
1304–1242	C-O bonds
1242–1178	Guaiacyl rings and C-O bonds
1167–1098	
1098–1061	
1061–989	
978–946	C-H of aromatic rings
946–900	
885–839	
832–773	

Table S 5: solubility tests on kraft lignin: 200 mg of kraft lignin were stirred in 100 mL of solvent, after 48 hours the solvent was filtered and the precipitated lignin was weighted to calculate the concentration of biopolymer dissolved, the lignin dissolved was also isolated and weighted after drying of the solvent. ^aTHF = tetrahydrofuran, GVL = γ -valerolactone, meTHF = 2-methyltetrahydrofuran.

Solvent	Concentration (mg mL ⁻¹)
MeOH	1.43
Water	0.23
EtOH	0.83
THF ^a	1.44
Dioxane	1.45
GVL ^a	>3
GVL:meTHF ^a (1:4)	>2

Table S 6: size exclusion chromatography and detected molecular weight of unreacted and reacted lignin after chromatographic column. Please refer to Table 2 in the manuscript for information regarding the depolymerisation conditions.

Entry (Table2)		DETECTOR					
		UV-1000-270nm			Shodex RI-71		
		Mn (g mol ⁻¹)	Mw (g mol ⁻¹)	Mz (g mol ⁻¹)	Mn (g mol ⁻¹)	Mw (g mol ⁻¹)	Mz (g mol ⁻¹)
1	Unreacted lignin	1930	4565	10198	2066	4593	9155
2	1 st fraction	363	647	1108	585	838	1204
	2 nd fraction	954	1908	3262	1466	2349	3657
	3 rd fraction		2834				
3	1 st fraction		682				
	2 nd fraction		1745				
	3 rd fraction	1326	2511	3897	1807	2835	3990
4	1 st fraction	553	720	828	502	603	728
	2 nd fraction	1287	2157	3437	1302	2219	3568
5	1 st fraction	493	606	749	507	608	737
	2 nd fraction	1109	1813	2727	1154	1846	2756
6	1 st fraction	562	737	905	497	603	735
	2 nd fraction	1248	1982	3178	1288	2069	3485
7	1 st fraction	512	650	824	526	645	804
	2 nd fraction	1398	1652	3654	1301	2577	3323
8	1 st fraction	655	711	910	616	758	863
	2 nd fraction	1254	1988	3425	1284	2245	3152
9	1 st fraction	541	689	752	598	656	812
	2 nd fraction	1157	2014	3541	1161	2085	3451
10	1 st fraction	499	652	712	515	623	764
	2 nd fraction	1541	1847	3178	1666	2178	3310

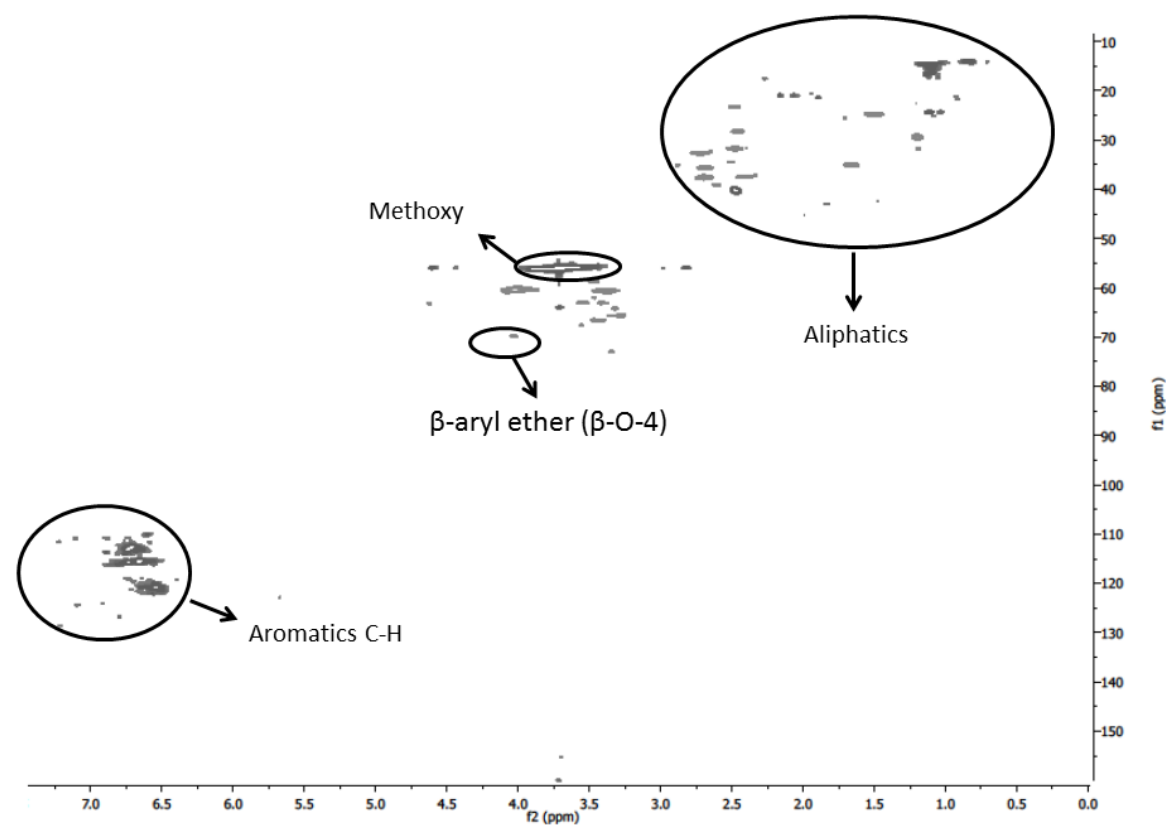


Figure S 8: 2D HSQC NMR analysis of fraction 1 of depolymerised lignin (Table 2, entry 3).

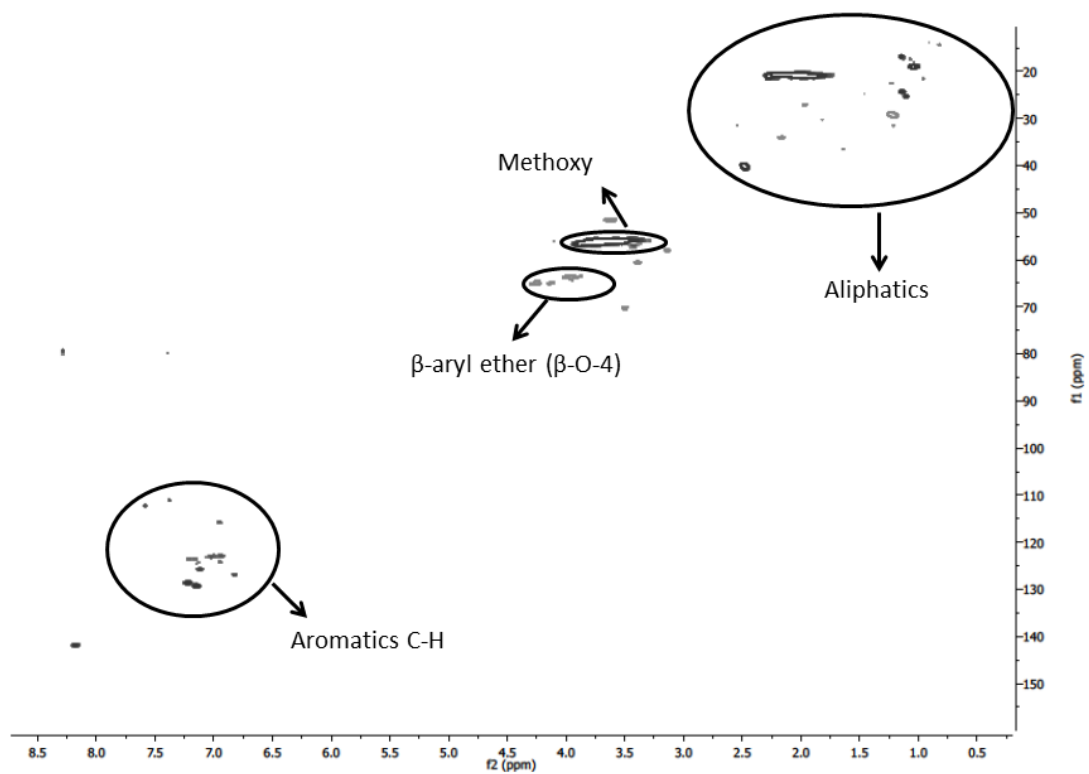


Figure S 9: 2D HSQC NMR analysis of acetylated kraft lignin (kraft lignin was acetylated before NMR analysis to improve its solubility).

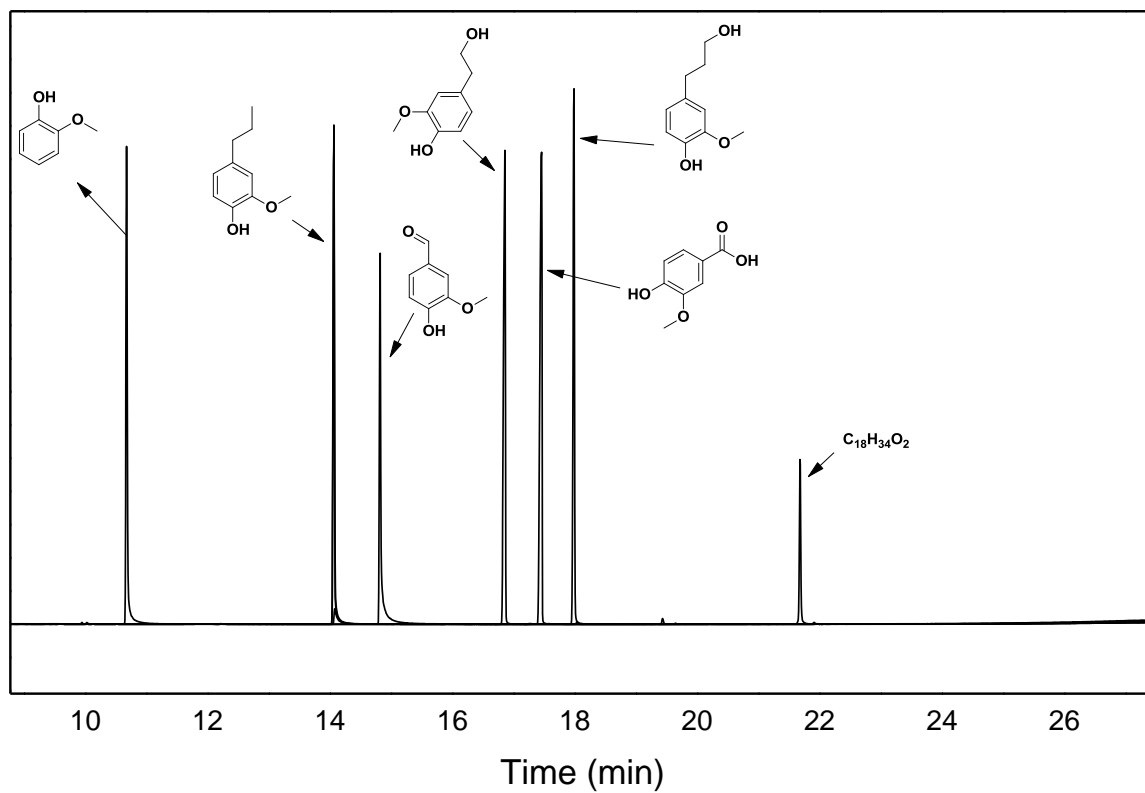


Figure S 10: molecules used as standard for the identification of the monomers produced via lignin hydrogenolysis.

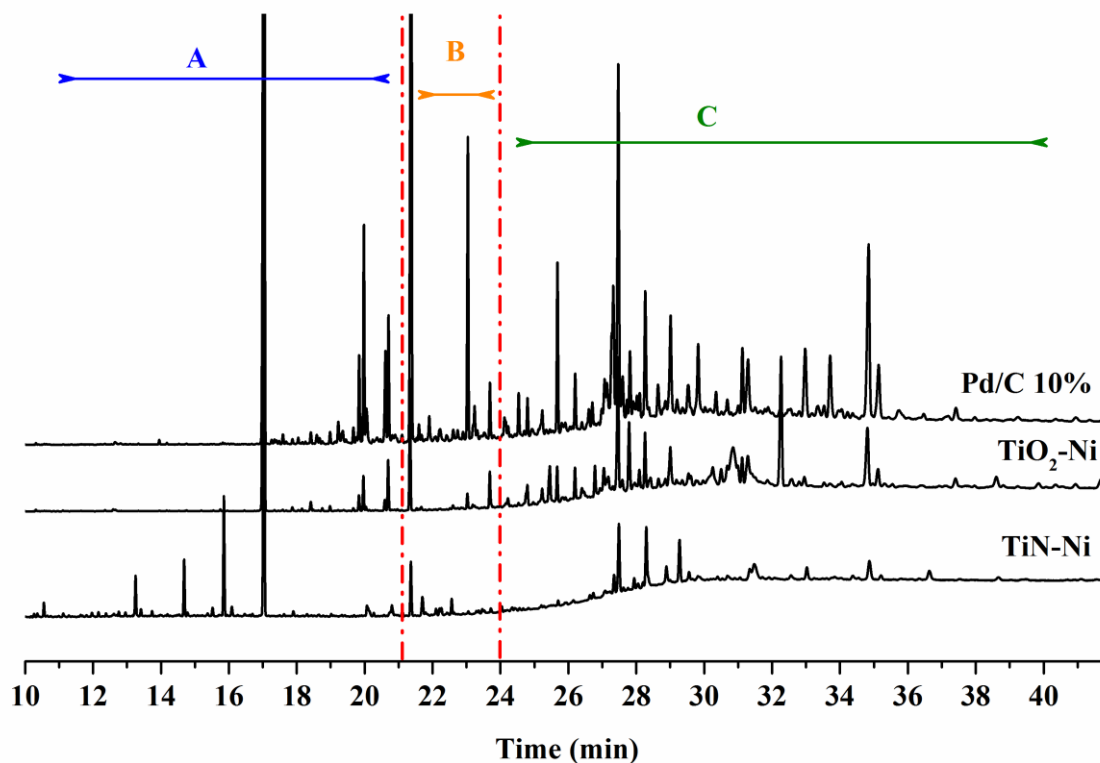


Figure S 11: GC-FID chromatograms of the depolymerized mixtures (fraction 1) obtained after lignin hydrogenation at 150 °C using Pd/C, TiO₂-Ni (50%) and TiN-Ni (50%) as catalysts.

Comments on Figure S11:

After a qualitative analysis of the mixtures (fraction 1) by GC-MS, quantification was performed on the GC-FID system. For convenience, the chromatogram was separated in three regions: the first one (A) contains all peaks between 10 and 21 min (quantification for compounds in this range was performed using the response factor and calibration curve calculated for guaiacol); the second one (B) contains all peaks between 21 and 24 min (quantification for compounds in this range was performed using the response factor and calibration curve calculated for hydrogenated coniferyl alcohol). The third one (C) contains all peaks between 24 and 40 min, usually containing molecules with more than 1 aromatic ring (quantification for compounds in this range was performed using the response factor and calibration curve calculated for 3-phenoxyphenol).

A qualitative comparison of the three chromatograms shows a different composition of the mixtures. A predominance of small molecules (A region) is obtained using TiN-Ni as catalyst. The cumulative area of regions B and C is bigger in the case of lignin hydrogenolysis performed with Pd/C and, interestingly, in the case of TiO₂-Ni catalyst, the majority of the signals are found in region C.

The results are confirmed by a quantitative characterization of the products. In case of TiN-Ni, the percentage of region A is 32.4 wt %, the one of B is 23.2 wt % while the region C represents the 44.5 wt % of the total area. A quantitative GC-FID analysis was performed in the same fashion for the mixtures (fraction 1) obtained by treatment of lignin with Pd/C and TiO₂-Ni (Table S7).

Table S 7: cumulative percent area for regions A, B and C (as defined in Comments on Figure S11) in the GC-FID chromatograms for the hydrogenolysis of lignin with different catalysts (Table 2).

Catalyst	A (%)	B (%)	C (%)
TiN-Ni	32.4	23.2	44.5
TiO ₂ -Ni	5.1	13.9	81.0
Pd/C	10.4	35.5	54.1

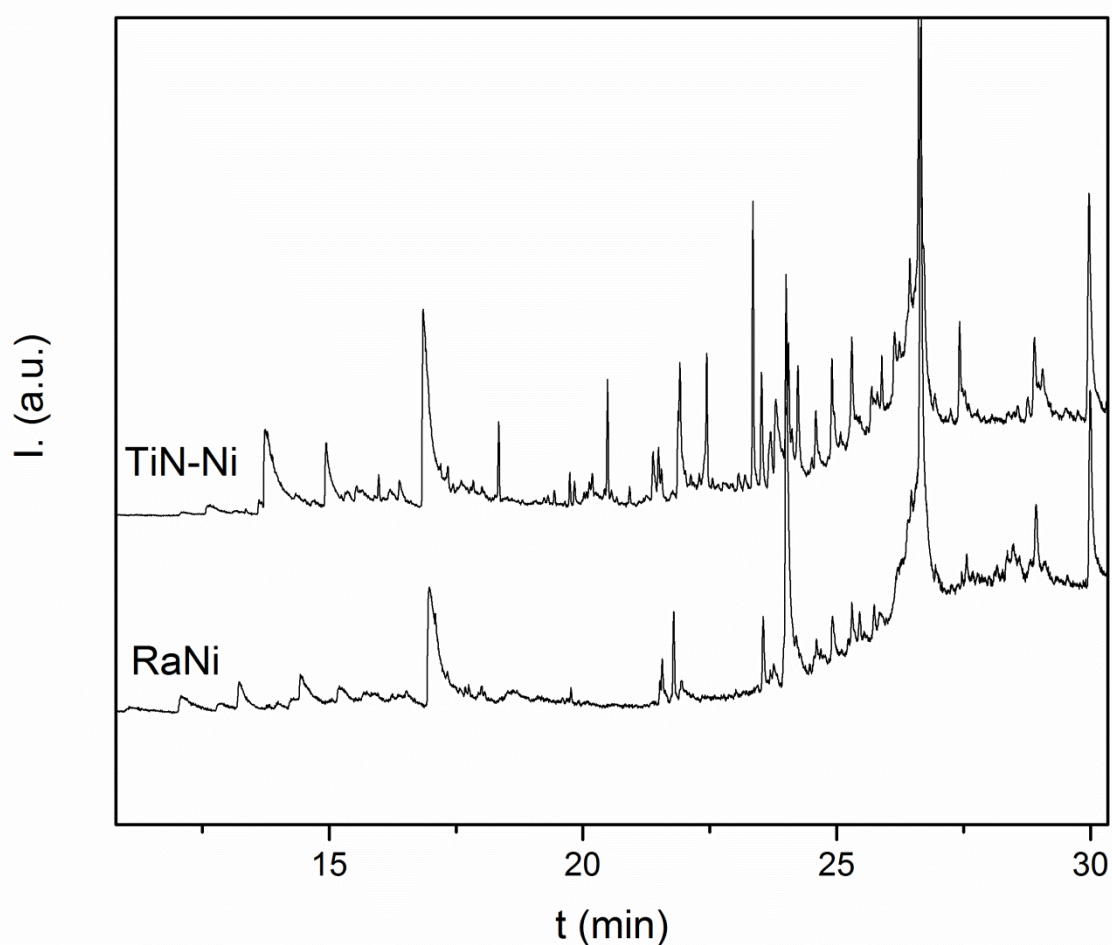


Figure S 12: GC-MS chromatograms of the depolymerized mixtures (fraction 1) obtained after lignin hydrogenation at 150 °C using TiN-Ni (50%) and RaNi as catalysts. Samples injected without derivatisation.

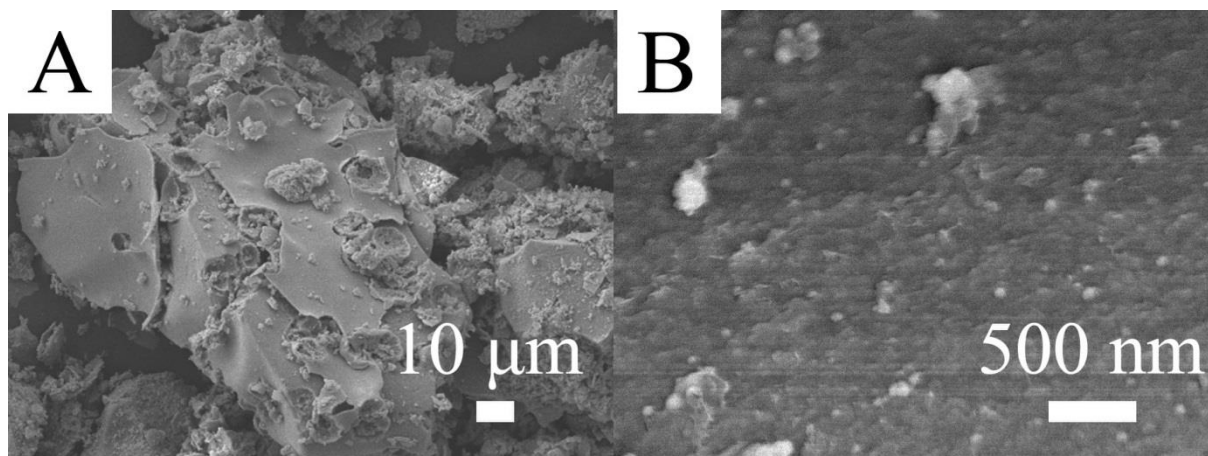


Figure S 13: SEM of TiN-Ni recovered after 500 hours of lignin hydrogenolysis (A), and high magnification (B).

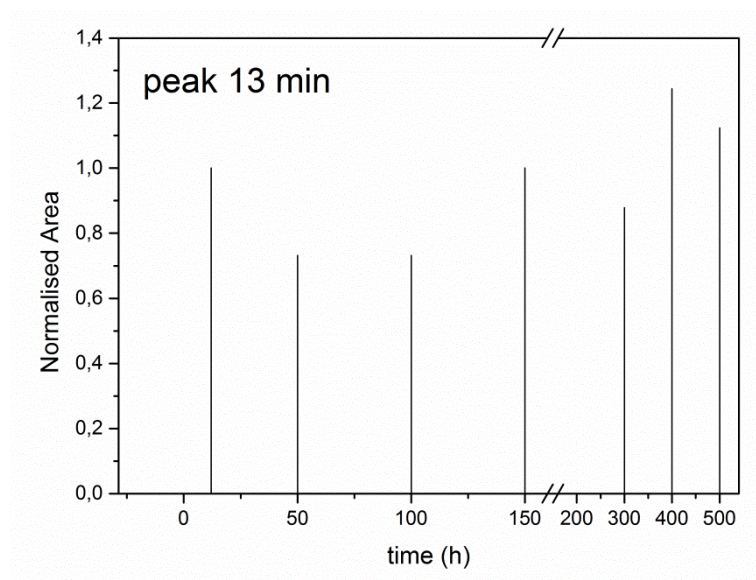


Figure S 14: normalized yields for 2-Methoxy-4-propylphenol (Figure 6A, peak at 13min) as a function of the time. The sample was injected without derivatisation of the –OH functional groups.

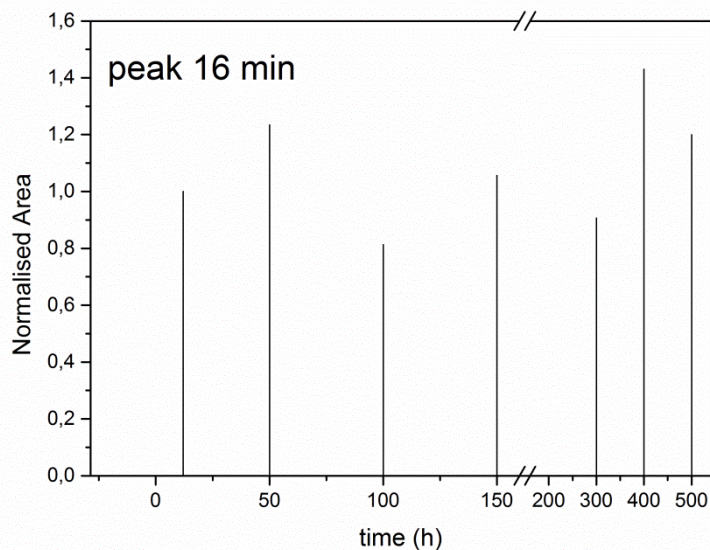


Figure S 15: normalized yields for Homovanillyl alcohol (Figure 6A, peak at 16 min). The sample was injected without derivatisation of the –OH functional groups.

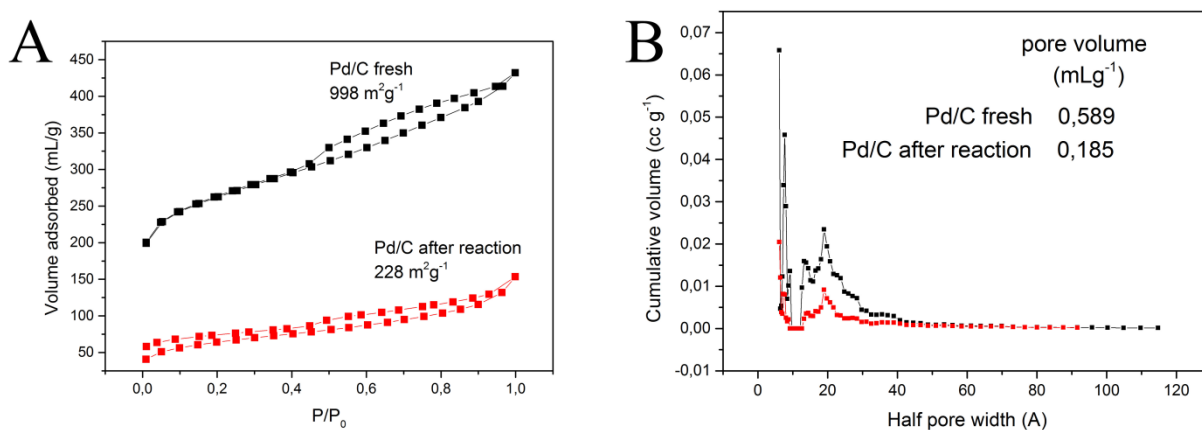


Figure S 16: Nitrogen sorption analysis and specific surface area (BET) of fresh and recovered Pd/C (A) and corresponding pore size distributions (B).

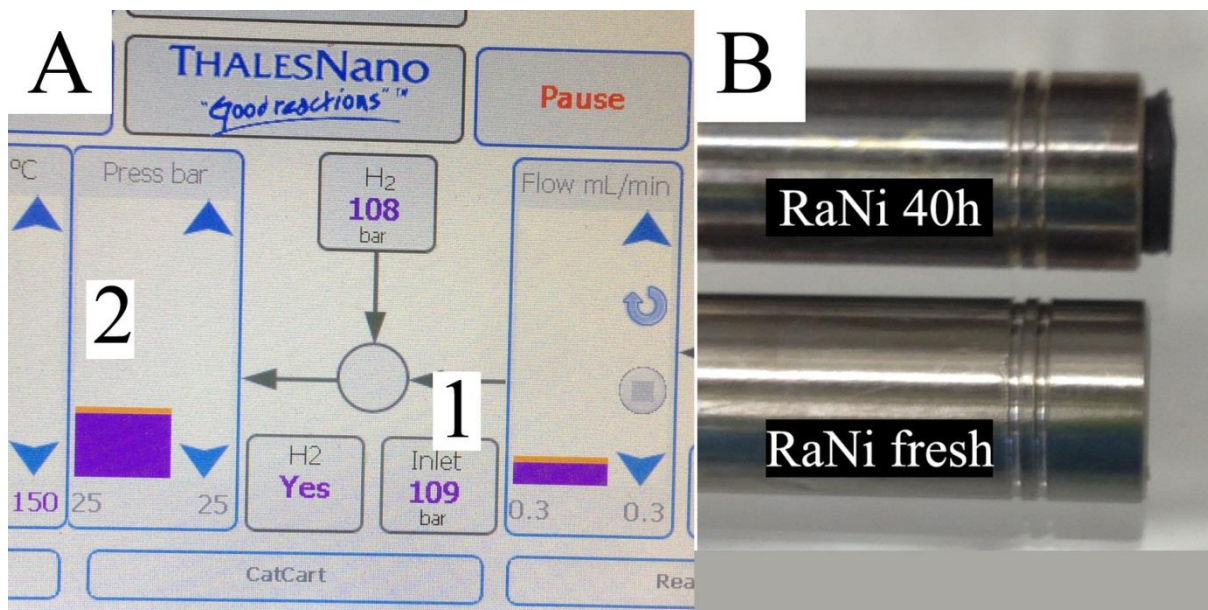


Figure S 17: screenshot of the flow system control panel indicating the pressure reached by the system (1) and the pressure set by the user (2) for the stability test with Raney Ni (A). RaNi leakage after 40 hours of reaction (B).

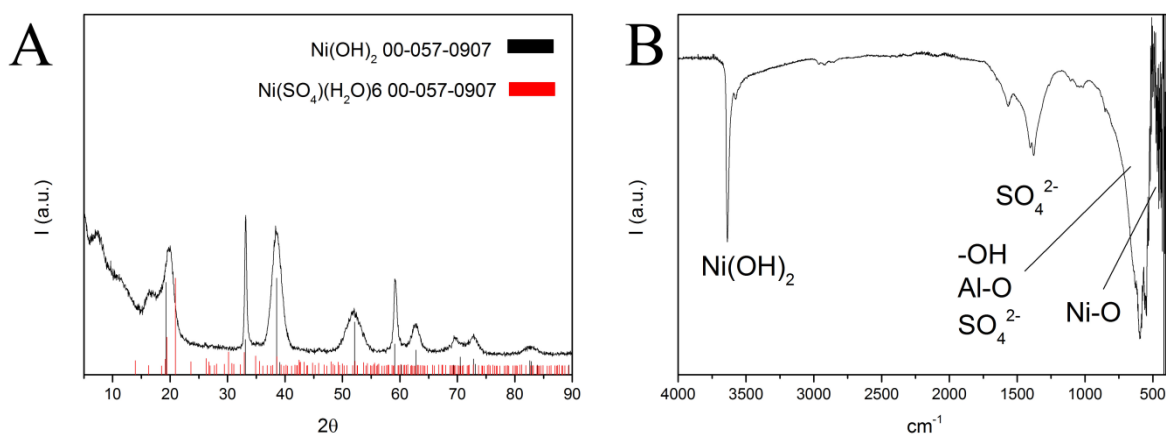


Figure S 18: diffractogram (A) and FTIR (B) of the powder leaked from RaNi catalytic bed.

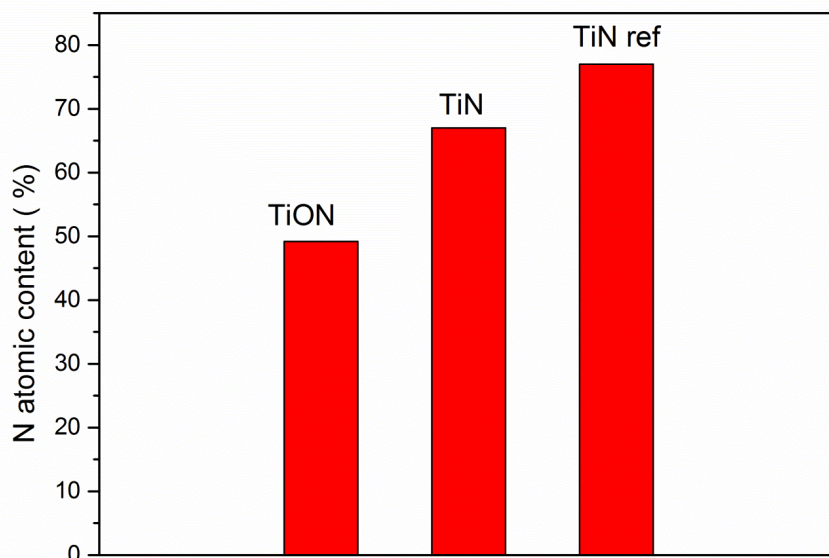


Figure S 19: Nitrogen atomic content quantified by Electron Energy Loss Spectroscopy in TiN prepared via urea route and on TiON and TiN reference samples.

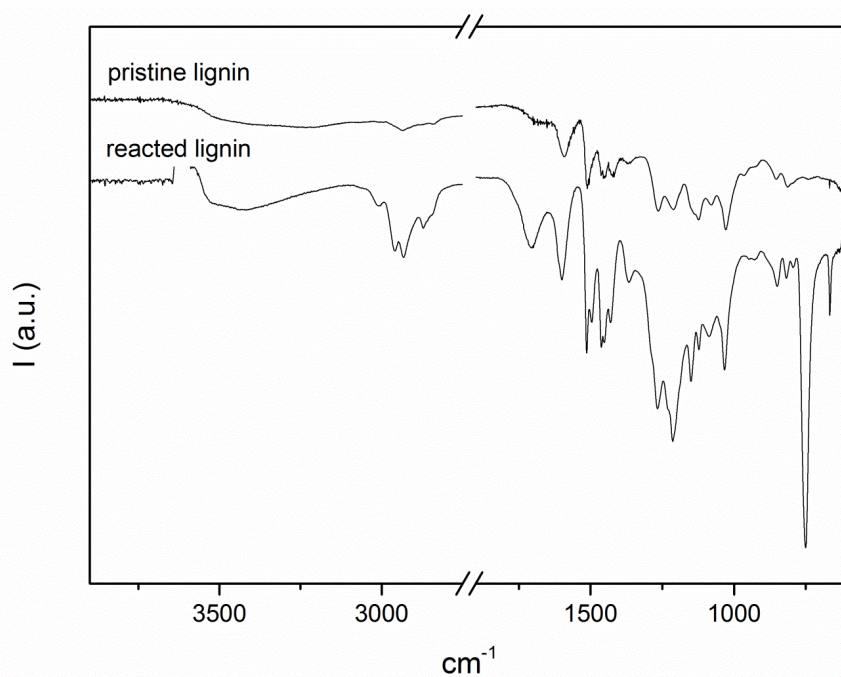


Figure S 20: FTIR of pristine and reacted lignin.

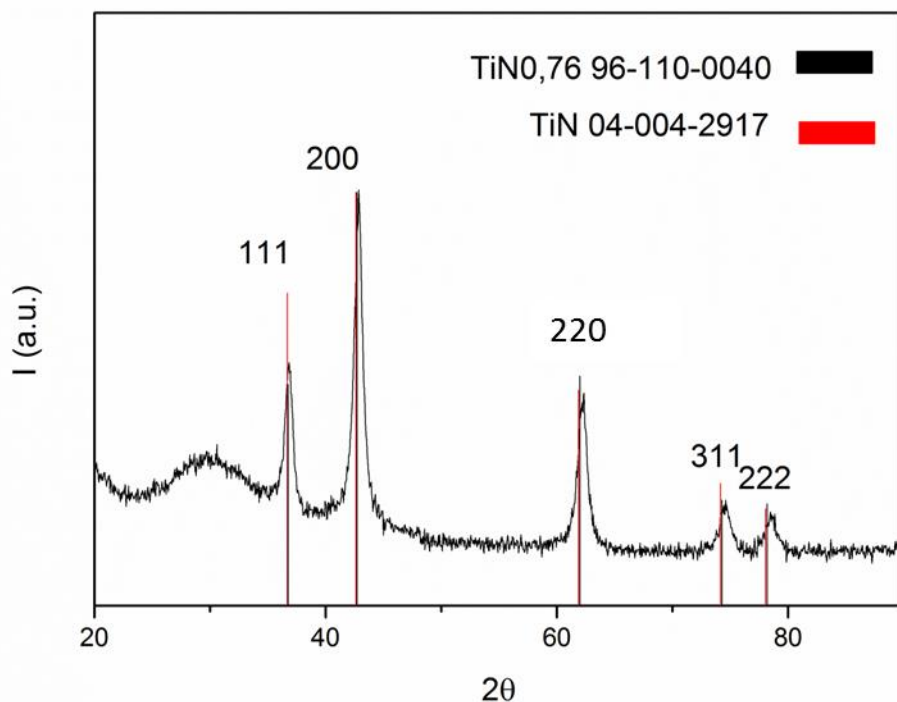


Figure S 21: Diffractogram of TiN prepared via urea route.

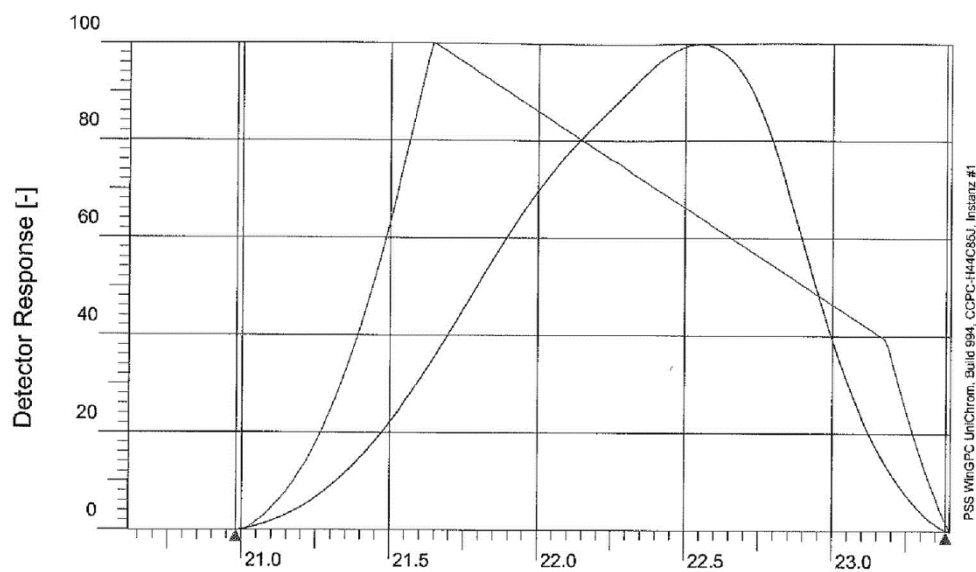


Figure S 22: Size Exclusion Chromatography of reacted lignin after reaction (Table 2, entry 2, Fraction 1).

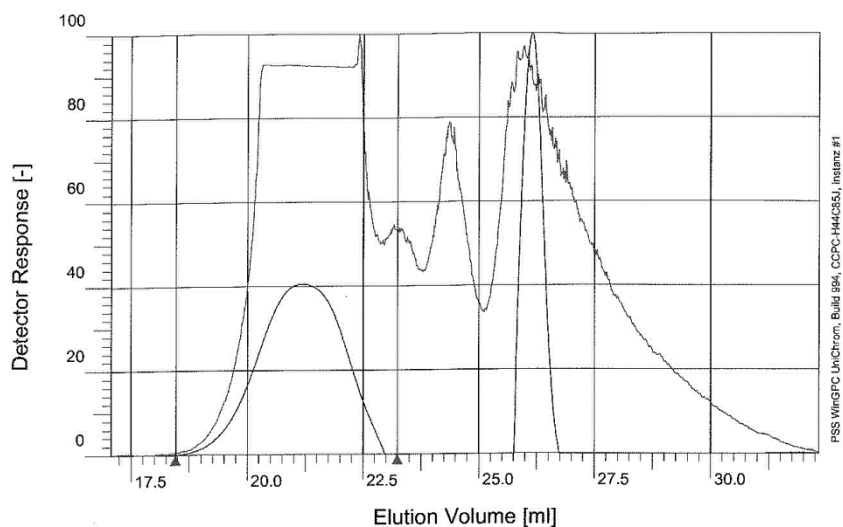


Figure S 23: Size Exclusion Chromatography of reacted lignin after reaction (Table 2, entry 2, Fraction 2), peak 25.5 mL (elution volume) is the signal of the internal standard.

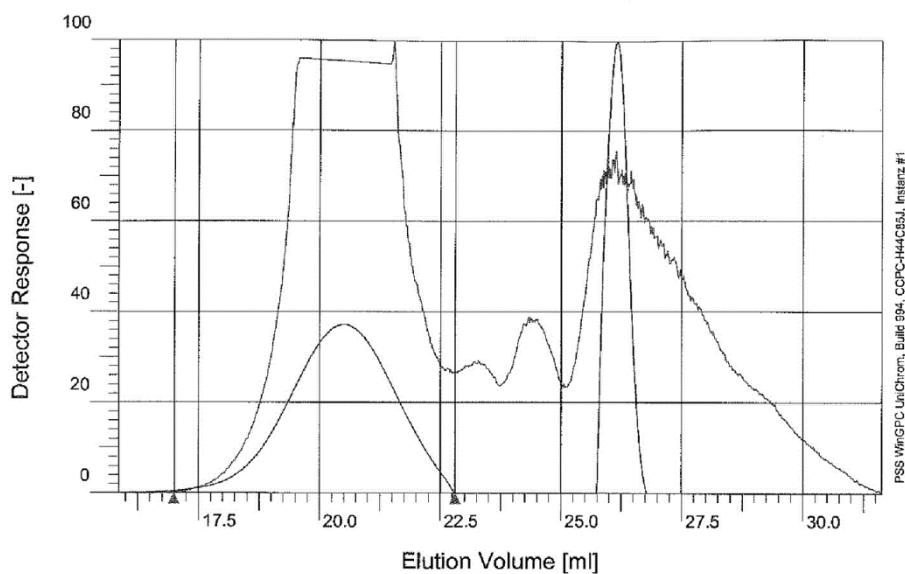


Figure S 24: Size Exclusion Chromatography of reacted lignin after reaction (Table 2, entry 2, Fraction 3), peak 25.5 mL (elution volume) is the signal of the internal standard.

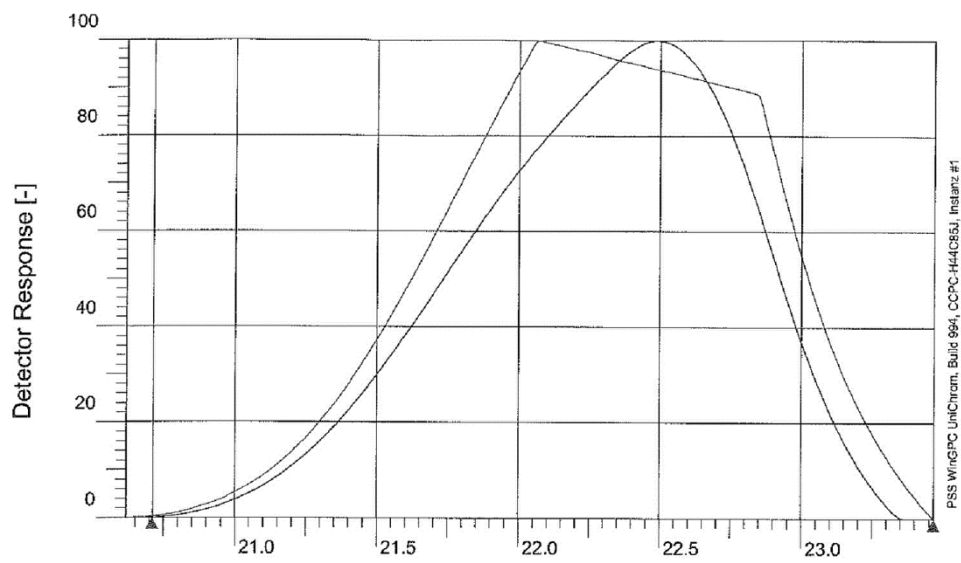


Figure S 25: Size Exclusion Chromatography of reacted lignin after reaction (Table 2, entry 3, Fraction 1).

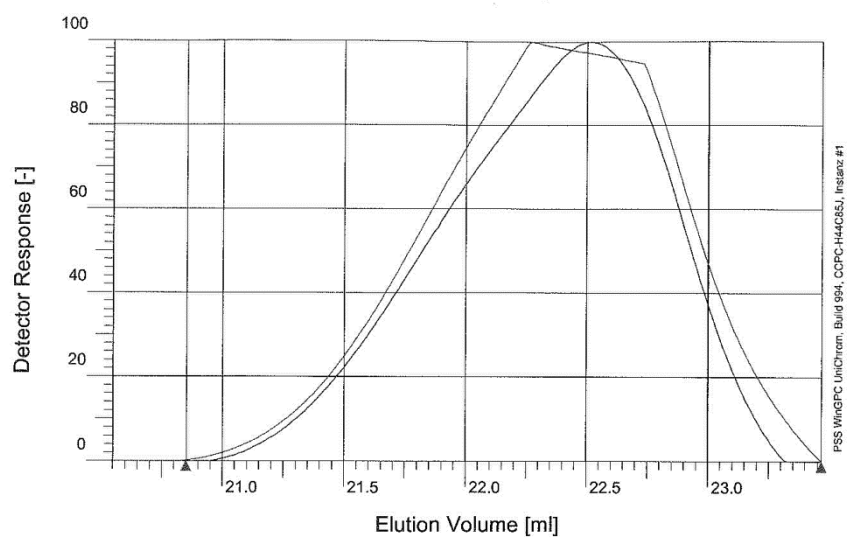


Figure S 26: Size Exclusion Chromatography of reacted lignin after reaction (Table 2, entry 5, Fraction 1).

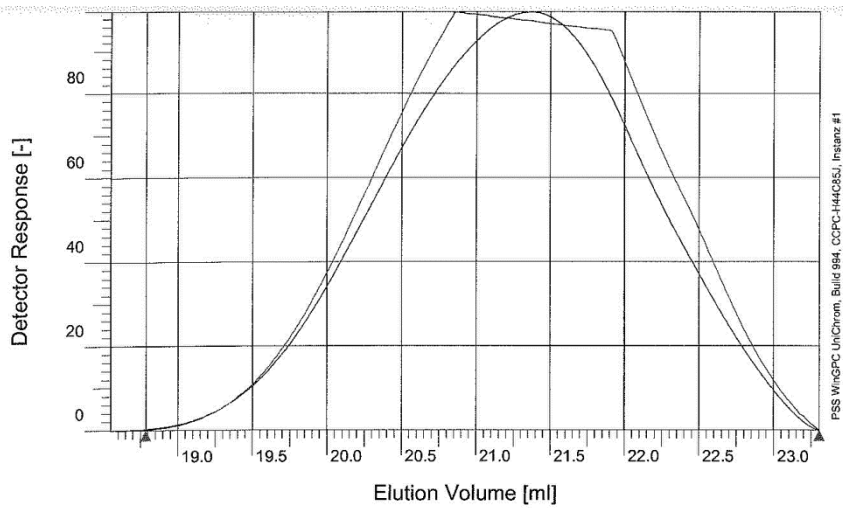


Figure S 27: Size Exclusion Chromatography of reacted lignin after reaction (Table 2, entry 5, Fraction 2).

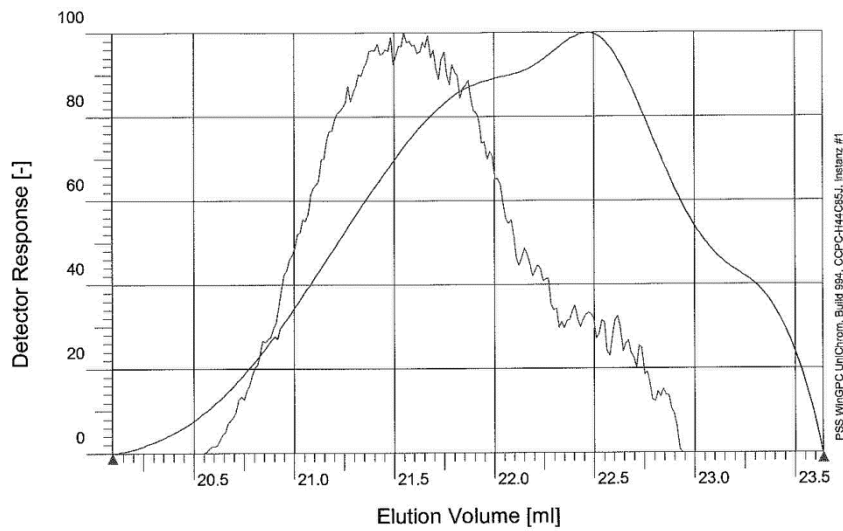


Figure S 28: Size Exclusion Chromatography of reacted lignin after reaction (Table 2, entry 9, Fraction 1).

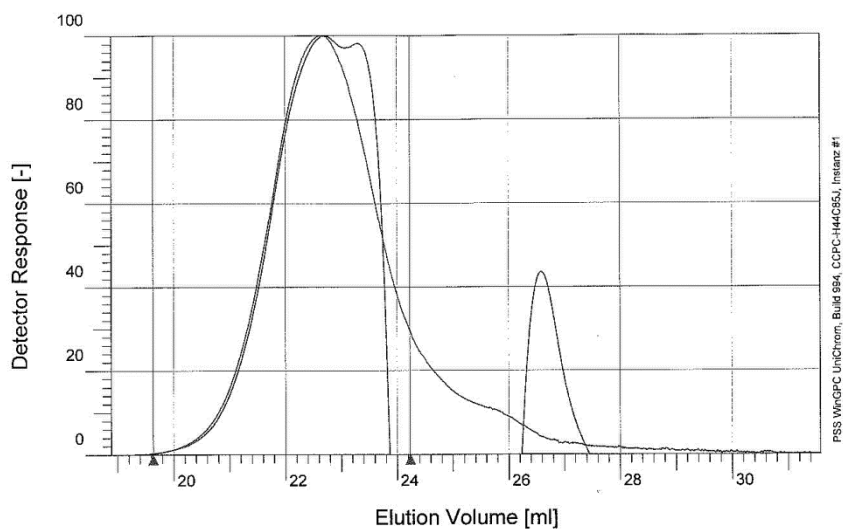


Figure S 28: Size Exclusion Chromatography of reacted lignin after reaction (Table 2, entry 13, fraction 1), peak at 26 mL (elution volume) is the signal of the internal standard.

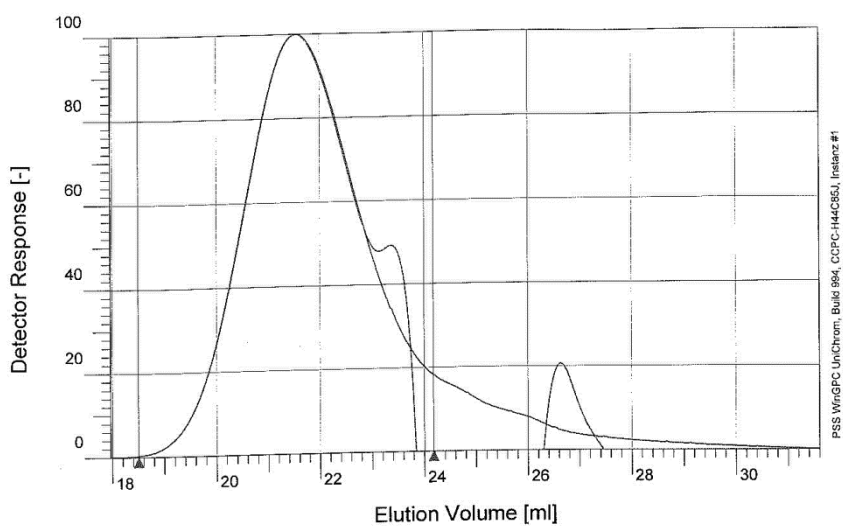


Figure S 30: Size Exclusion Chromatography of reacted lignin after reaction (Table 2, entry 13, fraction 2), peak at 26 mL (elution volume) is the signal of the internal standard.

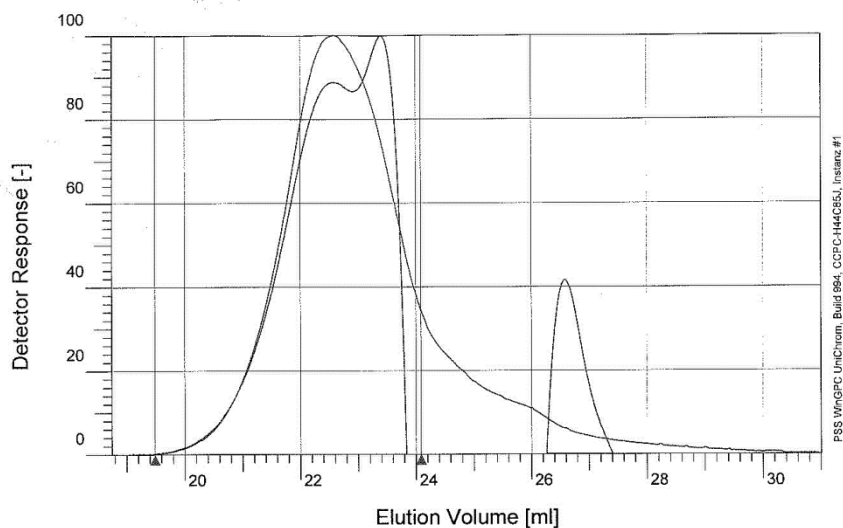


Figure S 31: Size Exclusion Chromatography of reacted lignin after reaction (Table 2, entry 14, fraction 1), peak at 26 mL (elution volume) is the signal of the internal standard.

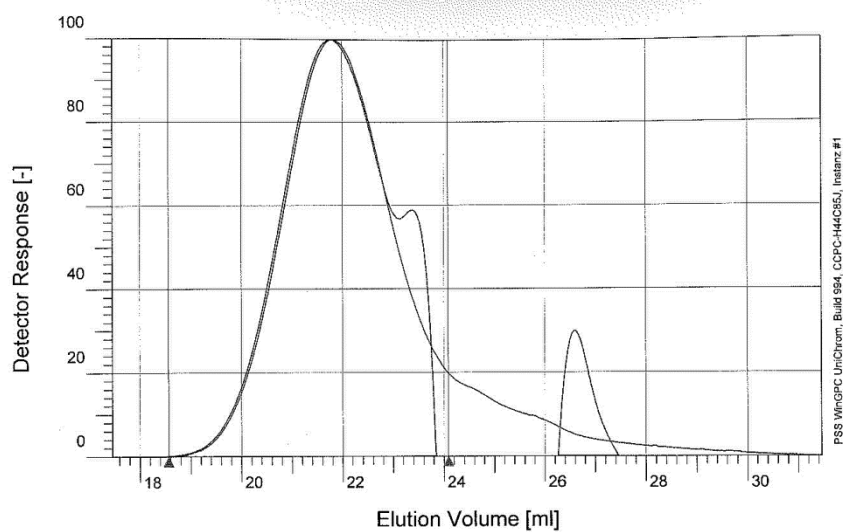


Figure S 29: Size Exclusion Chromatography of reacted lignin after reaction (Table 2, entry 14, fraction 2), peak at 26 mL (elution volume) is the signal of the internal standard.